Local Shocks, Global Ripples: Climate Disruptions in Maritime Trade Networks

Jeisson Prieto

Charles H. Dyson School of Applied Economics and Management

Midwest Trade & Theory 2026

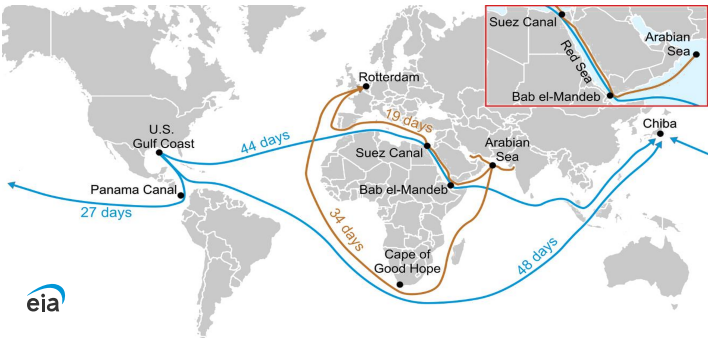


Trade and Climate Adaptation

- Climate shocks affect productivity, economic growth, and the geography of economic activity [Dell et al., 2012, Cruz and Rossi-Hansberg, 2024].
- Trade can moderate climate damages by allowing economies to adjust sourcing and production across locations and sectors [Gouel and Laborde, 2021, Rudik et al., 2022, Nath, 2025].

- But these adjustments depend on transportation networks: around 80% of international trade in goods, by volume, travels by sea [UNCTAD, 2024].
- Climate shocks can also disrupt shipping routes and ports, transmitting economic losses through trade networks:
  - Arctic route openings [Bekkers et al., 2018]
  - Sea-level threats to ports [Hanson and Nicholls, 2020]
  - Weather disruptions [Dunbar et al., 2023, Feng et al., 2025].

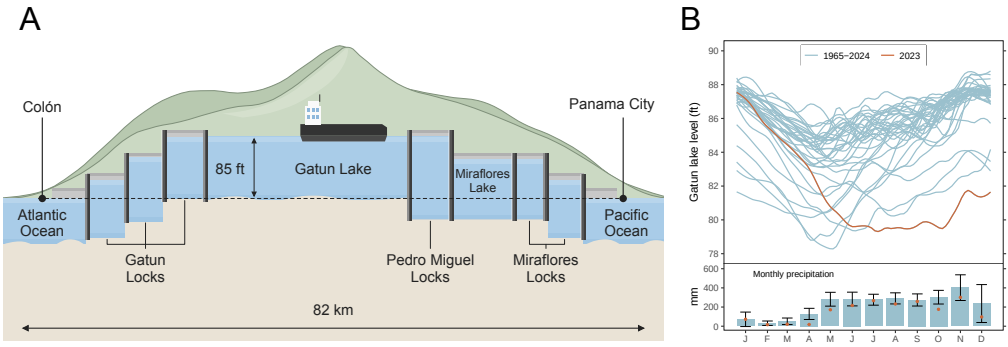
Chokepoints and the Reordering of Global Trade



Source: U.S. Energy Information Administration (2024)

- Global trade routes depend on maritime chokepoints [Känzig and Raghavan, 2025]
- Most disruptions are geopolitical or accidental—but **the Panama Canal capacity is governed by freshwater availability** in Gatun Lake

The Panama Canal Hub



- Operates via a **lock system** fed by Gatun Lake—link between hydrology and capacity
- **2023–2024 Drought** ⇒ FY2024 transits ↓ **29.3%** (vs. FY2023) [PCA, 2026].
- Handles ∼5% of world trade; 15% of U.S. waterborne foreign trade [BTS, 2024]

Research question

How does a climate-induced reduction in shipping capacity at a critical transportation node propagate through global trade networks?

I trace its effects through four stages:

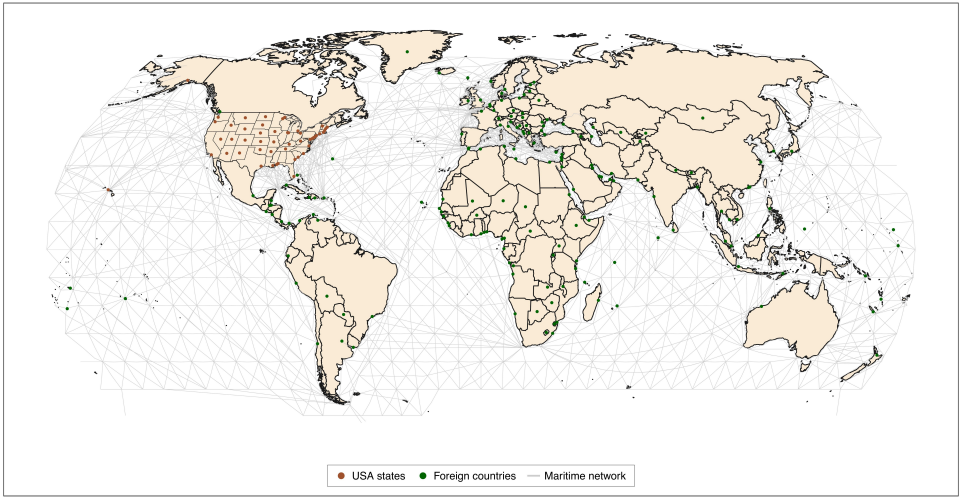
- **Canal capacity:** Estimate how low-water exposure affects Canal operations.
- **Trade and rerouting:** Estimate trade responses to low water by Canal dependence and document rerouting.
- **Network propagation:** Use a network trade model to quantify changes in trade costs and market access.
- **Welfare incidence:** Quantify welfare effects across economies.

Data Sources

- **Canal Operations**†: Panama Canal Authority (1990–2025) ▸ Detail
  - Transit statistics (2003–2025): transits, booked/auctioned slots, toll revenue, net tonnage
  - Hydrological & Meteorological‡: lake levels, inflows, runoff precipitation, temperature
- **Trade Flows**†: U.S. Census Bureau & UN Comtrade (2010–2025) ▸ Detail
  - U.S. imports and exports by state and commodity.
  - Bilateral trade by product and partner: 166 countries
- **Maritime Network**: IMF Port Watch & Eurostat–Marnet ▸ Detail
  - Representative ports and global sea routes [Shen et al., 2020]
  - ∼14,000-node routing graph — least-cost paths via Dijkstra algorithm
- **AIS Vessel Movements**‡: Global Fishing Watch (2012–2026) ▸ Detail
  - Global cargo and tanker port visits and vessel identities
  - ∼11 million harmonized port-to-port movements across ∼30,000 vessels

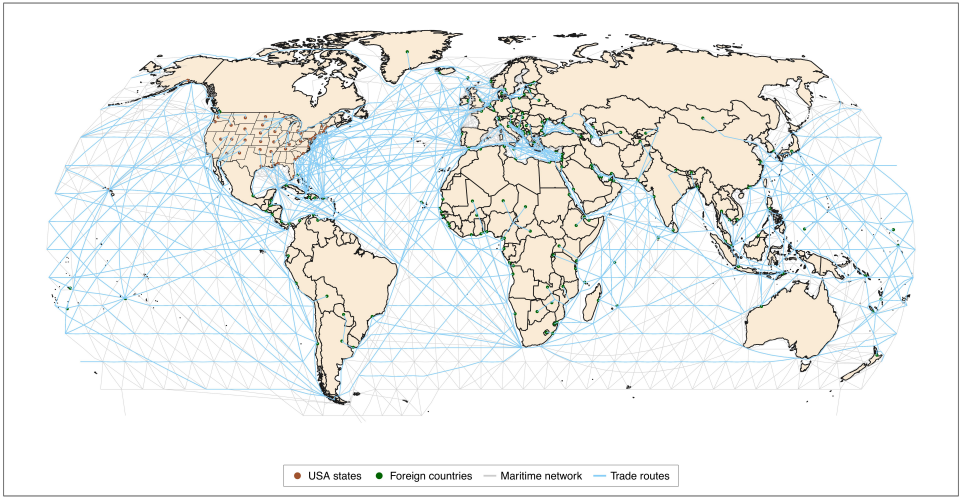
†: Monthly frequency, ‡: Daily frequency.

Maritime Trade Routes



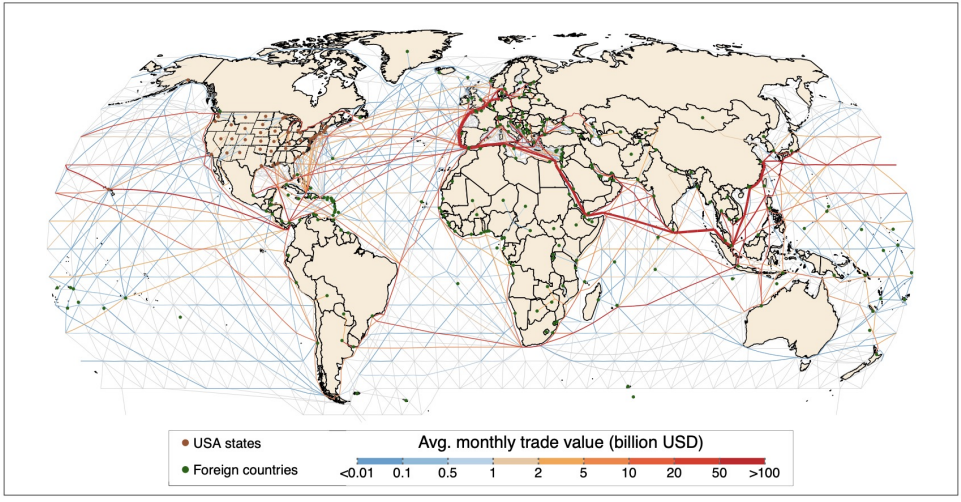
back

Maritime Trade Routes



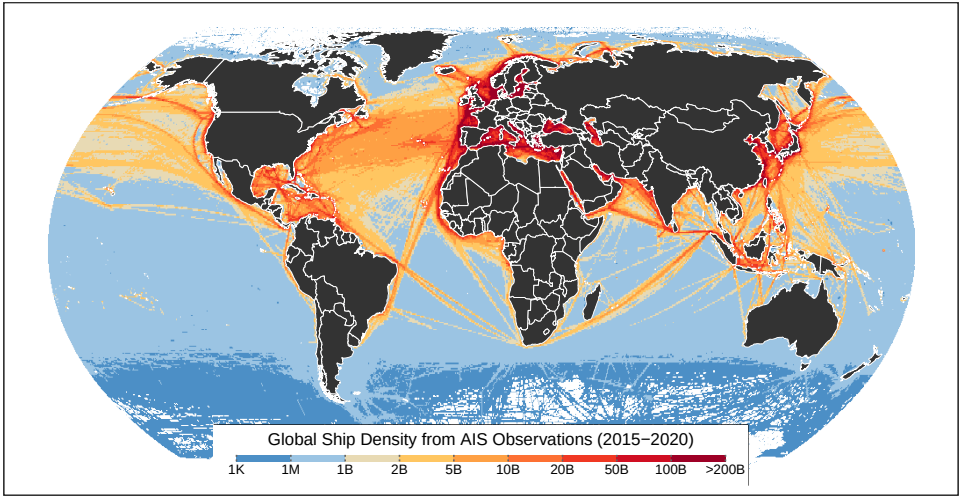
back

Maritime Trade Routes



back

Global Shipping Traffic Density



Source: World Bank

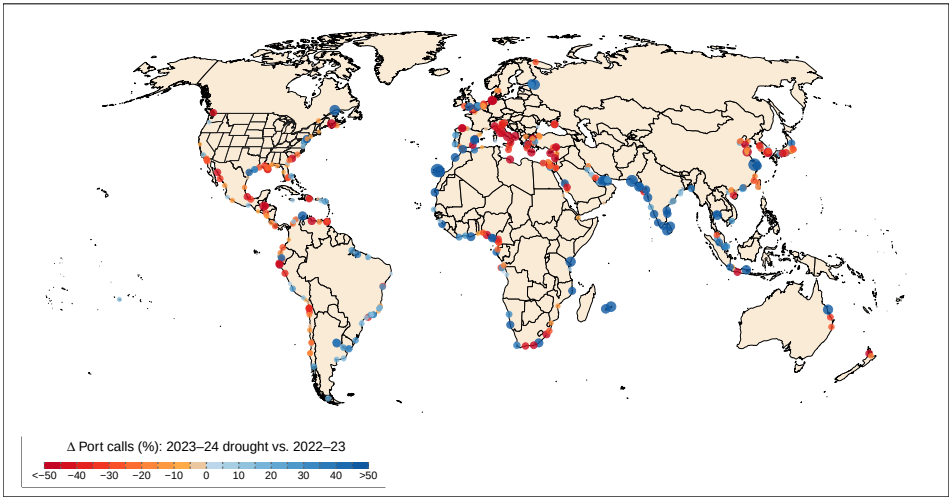
back

Data Sources

- **Canal Operations**†: Panama Canal Authority (1990–2025) ▸ Detail
  - Transit statistics (2003–2025): transits, booked/auctioned slots, toll revenue, net tonnage
  - Hydrological & Meteorological‡: lake levels, inflows, runoff precipitation, temperature
- **Trade Flows**†: U.S. Census Bureau & UN Comtrade (2010–2025) ▸ Detail
  - U.S. imports and exports by state and commodity.
  - Bilateral trade by product and partner: 166 countries
- **Maritime Network**: IMF Port Watch & Eurostat–Marnet ▸ Detail
  - Representative ports and global sea routes [Shen et al., 2020]
  - ∼14,000-node routing graph — least-cost paths via Dijkstra algorithm
- **AIS Vessel Movements**‡: Global Fishing Watch (2012–2026) ▸ Detail
  - Global cargo and tanker port visits and vessel identities
  - ∼11 million harmonized port-to-port movements across ∼30,000 vessels

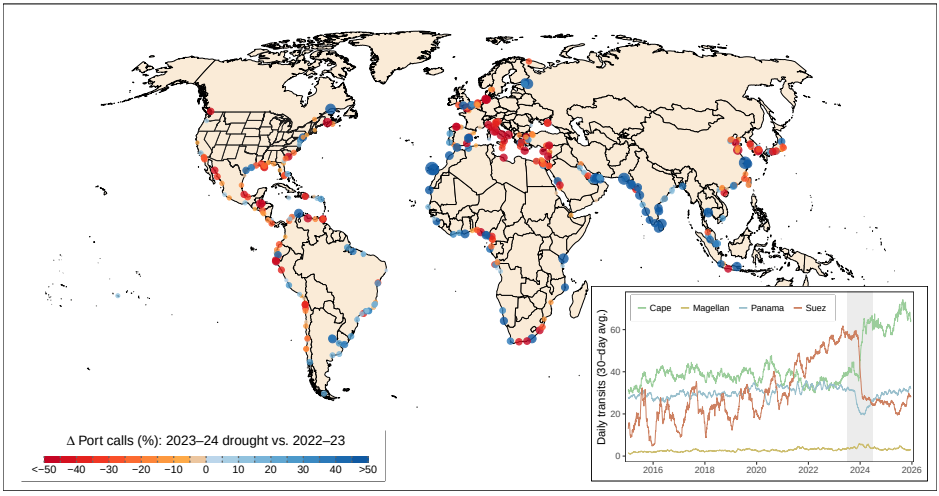
†: Monthly frequency, ‡: Daily frequency.

AIS Vessel Movements



back

AIS Vessel Movements

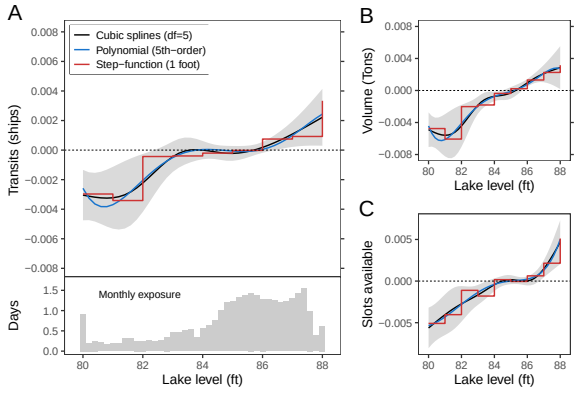


back

Lake-Level Exposure and Canal Operations

$$y_t = \int_{\underline{l}}^{\bar{l}} g(l)\phi_t(l)dl + \psi(t) + \varepsilon_t$$

- y_t is the oceangoing traffic at month t
- $g(l)$ is the potentially non-linear effect of lake level l on traffic
- $\phi_t(l)$ is the within-month distribution of daily lake levels
- $\psi(t)$ is the monthly trend capturing seasonal patterns
- ε_t is the error term.



Notes: Cubic spline baseline; shaded 90% CIs; Newey–West SEs (L=4).

Capacity Constraints and Rationing Mechanisms

	Transits (ships/mth)	Volume (Tons/mth)	Toll revenue (USD/mth)	Rev/Transit (USD/ship)	Slots available
Days below 82 ft	-0.0029***	-0.0044***	-0.0023***	0.0006*	-0.0040***
	(0.0010)	(0.0012)	(0.0008)	(0.0003)	(0.0014)
Days above 86 ft	0.0010	0.0022**	0.0009	-0.0001	0.0014*
	(0.0007)	(0.0009)	(0.0006)	(0.0004)	(0.0008)
Below 82 ft (%)					
+10 days	-2.88	-4.26	-2.30	0.60	-3.88
+30 days	-8.40	-12.24	-6.74	1.82	-11.20
Observations	267	267	267	267	267

Notes: Reference regime: 82–86 ft; Newey–West SEs (L=4); $^{*}p < 0.10$, $^{**}p < 0.05$, $^{***}p < 0.01$.

- +30 days below 82 ft reduces **Canal transits by 8.4%** and cargo volume by **12.2%**.
- The pattern is consistent with adjustment through **quantity restrictions**: slots available decline by 11.2%, while revenue per transit rises 1.8%. ▸ Detail

Days Below 82ft: $D_t^{<82} \equiv \sum_{d \in \mathcal{D}_t} \mathbf{1}\{l_{dt} < 82\}$, where l_{dt} is the daily Gatún Lake level.

Bilateral Trade Response to Canal Water Scarcity

$$\mathbb{E}[X_{ijt} \mid \cdot] = \exp\left[\underbrace{\left(\beta_L\, D_t^{<82} + \beta_H\, D_t^{>86}\right) \times \kappa_{ij}^{PC}}_{\text{Water regime} \times \text{PC dependence}} + \underbrace{\mu_{ij}}_{\text{Pair FE}} + \underbrace{\eta_{it} + \zeta_{jt}}_{\text{Exp./Imp.} \times \text{time FE}} + \underbrace{\psi_{PC}(t)}_{\text{Seasonal} \times \text{PC dep.}}\right]$$

Following [Heiland et al., 2025]: $\kappa_{ij}^{PC} \equiv \log(D_{ij}^{\text{NoPC}} / D_{ij}^{\text{Base}})$ measures the proportional increase in shortest-route distance when Panama is unavailable (e.g., New York-China: 17% farther, while New York-New Zeland: 59% farther without Panama).

Bilateral Trade Response to Canal Water Scarcity

$$\mathbb{E}[X_{ijt} \mid \cdot] = \exp\left[\underbrace{\left(\beta_L\, D_t^{<82} + \beta_H\, D_t^{>86}\right) \times \kappa_{ij}^{PC}}_{\text{Water regime} \times \text{PC dependence}} + \underbrace{\mu_{ij}}_{\text{Pair FE}} + \underbrace{\eta_{it} + \zeta_{jt}}_{\text{Exp./Imp.} \times \text{time FE}} + \underbrace{\psi_{PC}(t)}_{\text{Seasonal} \times \text{PC dep.}}\right]$$

	Global	U.S. Trade	
	Value	Value	Weight
Days below 82 ft $\times \kappa_{ij}^{PC}$	−0.0008**	−0.0007	−0.0025*
	(0.0004)	(0.0007)	(0.0013)
Days above 86 ft $\times \kappa_{ij}^{PC}$	0.0001	0.0003	0.0013
	(0.0005)	(0.0007)	(0.0012)
Num. Obs.	4,115,373	1,428,476	1,428,476

Notes: PPML estimates. Driscoll–Kraay SEs (L=6). $^{*}p < 0.10$, $^{**}p < 0.05$, $^{***}p < 0.01$.

- 30 days below 82 ft **reduces trade value by 0.4–1.2%**, depending on the detour.
- In U.S. data, the response is larger for **physical trade quantities** than for trade value.

Following [Heiland et al., 2025]: $\kappa_{ij}^{PC} \equiv \log(D_{ij}^{\text{NoPC}} / D_{ij}^{\text{Base}})$ measures the proportional increase in shortest-route distance when Panama is unavailable (e.g., New York-China: 17% farther, while New York-New Zeland: 59% farther without Panama).

AIS Evidence on Maritime Rerouting

$$\mathbb{E}[V_{ijgt} \mid \cdot] = \exp\left[\underbrace{\sum_{h \neq PC} \mathbf{1}\{g = h\}\left(\beta_{Lh} D_t^{<82} + \beta_{Hh} D_t^{>86}\right)}_{\text{Water regime} \times \text{alternative corridor}} + \underbrace{\mu_{ijg}}_{\text{OD} \times \text{corridor FE}} + \underbrace{\lambda_{ijt}}_{\text{OD} \times \text{time FE}} + \underbrace{\psi_g(t)}_{\text{Season} \times \text{corridor}}\right]$$

AIS Evidence on Maritime Rerouting

$$\mathbb{E}[V_{ijgt} \mid \cdot] = \exp\left[\underbrace{\sum_{h \neq PC} \mathbf{1}\{g = h\}\left(\beta_{Lh} D_t^{<82} + \beta_{Hh} D_t^{>86}\right)}_{\text{Water regime} \times \text{alternative corridor}} + \underbrace{\mu_{ijg}}_{\text{OD} \times \text{corridor FE}} + \underbrace{\lambda_{ijt}}_{\text{OD} \times \text{time FE}} + \underbrace{\psi_g(t)}_{\text{Season} \times \text{corridor}}\right]$$

	Alternative	Cape	Magellan	Suez
Days below 82 ft	0.0322**	0.0297**	0.0397**	0.0193
	(0.0130)	(0.0122)	(0.0174)	(0.0307)
Days above 86 ft	−0.0246*	−0.0165	−0.0484**	0.0203
	(0.0142)	(0.0135)	(0.0202)	(0.0296)
Observations	30,669	30,669	30,669	30,669

Notes: PPML estimates. Voyages are assigned to departure month. Sample restricted to Origin-Destination pairs observed using Panama and at least one alternative corridor. "Alternative" pools Cape, Magellan, and Suez into a single category. Driscoll–Kraay SEs (L=6). $^{*}p < 0.10$, $^{**}p < 0.05$, $^{***}p < 0.01$.

- Low-water conditions shift traffic **away from Panama toward alternative routes**.
- Reallocation is concentrated through **Cape and Magellan**.

Model: Trade on a Climate-Sensitive Network

- Countries connect through a **maritime network** $\mathcal{G} = (\mathcal{V}, \mathcal{E})$ of ports and transit nodes
- Firms choose the **least-cost route** across all feasible paths [Allen and Arkolakis, 2022]:

$$X_{ij} = \tau_{ij}^{-\theta} \frac{Y_i}{\Pi_i} \frac{E_j}{P_j}, \quad \tau_{ij} = \left(\sum_{r \in \mathcal{R}_{ij}} \prod_{(l,l') \in r} t_{ll'}^{-\theta} \right)^{-1/\theta}$$

Model: Trade on a Climate-Sensitive Network

- Countries connect through a **maritime network** $\mathcal{G} = (\mathcal{V}, \mathcal{E})$ of ports and transit nodes
- Firms choose the **least-cost route** across all feasible paths [Allen and Arkolakis, 2022]:

$$X_{ij} = \tau_{ij}^{-\theta} \frac{Y_i}{\Pi_i} \frac{E_j}{P_j}, \quad \tau_{ij} = \left(\sum_{r \in \mathcal{R}_{ij}} \prod_{(l,l') \in r} t_{ll'}^{-\theta} \right)^{-1/\theta}$$

- **Capacity at climate-sensitive nodes deteriorates under adverse local conditions**, raising baseline costs on affected links:

$$\bar{t}_{ll'}(\boldsymbol{\omega}) = \bar{t}^0_{ll'} \, \phi(\omega_l, \kappa_{ll'})$$

where ω_l measures climate stress at node l, $\kappa_{ll'} \in \{0, 1\}$ identifies exposed links, and

$$\phi(0, \kappa) = 1, \qquad \phi(\omega_l, 0) = 1, \qquad \partial \phi(\omega_l, 1)/\partial \omega_l > 0.$$

- Higher costs on constrained links $\Rightarrow$ **rerouting toward alternative paths**
- **Network spillovers** propagate to non-exposed routes and trading pairs

Calibration: Mapping Water Scarcity into Transport Costs

- **Equilibrium traffic on link (l, l'):**

$$\Xi_{ll',t} = \bar{t}_{ll',t}^{-\theta} \tilde{P}_{l,t}^{-\theta} \tilde{\Pi}_{l',t}^{-\theta}.$$

- **Panama transport costs respond to hydrological conditions:**

$$\bar{t}_{ll',t} = \bar{t}^0_{ll'} \exp\left[\mathbf{1}\{(l, l') \in \mathcal{E}_{PC}\} \left(\delta_L D_t^{<82} + \delta_H D_t^{>86}\right)\right]$$

- **Empirical analogue using AIS traffic:**

$$\mathbb{E}[\widehat{\Xi}_{ll't} \mid \cdot] = \exp\left[\mathbf{1}\{(l, l') \in \mathcal{E}_{PC}\} \left(\alpha_L D_t^{<82} + \alpha_H D_t^{>86}\right) + \mu_{ll'} + \eta_{lt} + \zeta_{l't} + \psi_{PC}(t)\right]$$

- **Mapping traffic into transport costs** [Heiland et al., 2025]:

$$\delta_L = -\alpha_L/\theta, \qquad \delta_H = -\alpha_H/\theta \qquad (\theta = 8).$$

Calibration: Mapping Water Scarcity into Transport Costs

- **Equilibrium traffic on link (l, l'):**

$$\Xi_{ll',t} = \bar{t}_{ll',t}^{-\theta} \tilde{P}_{l,t}^{-\theta} \tilde{\Pi}_{l',t}^{-\theta}.$$

- **Panama transport costs respond to hydrological conditions:**

$$\bar{t}_{ll',t} = \bar{t}_{ll'}^{0} \exp\left[\mathbf{1}\{(l, l') \in \mathcal{E}_{PC}\} \left(\delta_L D_t^{<82} + \delta_H D_t^{>86}\right)\right]$$

- **Empirical analogue using AIS traffic:**

$$\mathbb{E}[\widehat{\Xi}_{ll't} \mid \cdot] = \exp\left[\mathbf{1}\{(l, l') \in \mathcal{E}_{PC}\} \left(\alpha_L D_t^{<82} + \alpha_H D_t^{>86}\right) + \mu_{ll'} + \eta_{lt} + \zeta_{l't} + \psi_{PC}(t)\right]$$

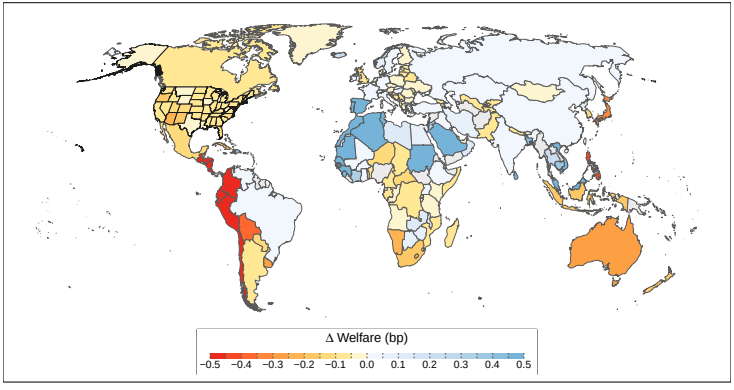
- **Mapping traffic into transport costs** [Heiland et al., 2025]:

$$\delta_L = -\alpha_L/\theta, \qquad \delta_H = -\alpha_H/\theta \qquad (\theta = 8).$$

- **Calibrated low-water shock $\hat{\alpha}_L = -0.0109 \Rightarrow \hat{\delta}_L = 0.0014$** Detail:

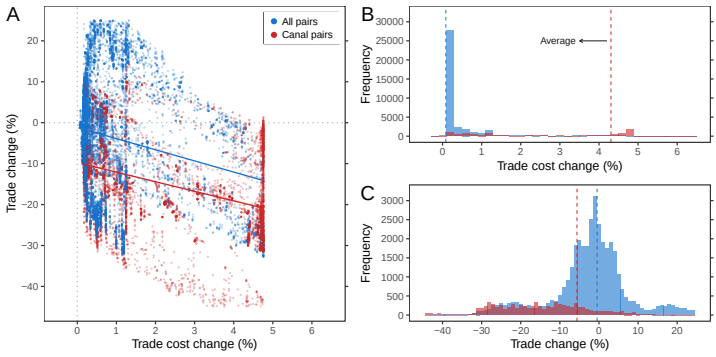
30 days below 82 ft implies **4.2% higher Panama transport costs**

Who Bears the Losses?



- *Counterfactual:* 30 days below 82 ft ▸ Method
- Deepest losses: Central America & Caribbean. All U.S. regions lose. ▸ Canal exposure
- Aggregate ≈ 0: **redistribution** with losses concentrated on Canal-dependent economies

Network Propagation in General Equilibrium



- Canal-dependent pairs face the largest **transport-cost increases and trade declines**.
- Endogenous rerouting **redistributes trade across the network**.
- The model implies a $\sim$**6% decline in trade**.

Conclusions

Main finding: Water scarcity at a single reservoir can generate global economic effects.

A full month below 82 ft:

- **Physical constraint:** Canal transits fall by **8.4%** and cargo volume by **12.2%**.
- **Trade and rerouting:** Bilateral trade falls by **0.4–1.2%**, depending on the detour required without the Canal; vessels shift toward **Cape and Magellan** routes.
- **Network propagation:** Panama transport costs rise by approximately **4.2%**; in general equilibrium, trade falls by approximately **6% for Canal-dependent pairs**.
- **Welfare incidence:** Losses are concentrated in **Central America and the Caribbean**; all U.S. regions lose; global aggregate masks redistribution across economies.

Future work

- Decompose network amplification: direct cost shock vs. rerouting spillovers
- Climate scenario extension: precipitation projections [Muñoz et al., 2025] $\Rightarrow$ Canal capacity $\Rightarrow$ welfare under climate change

Thank you!

Any questions?



Jeisson Prieto
jp2276@cornell.edu
jeissonprieto.com

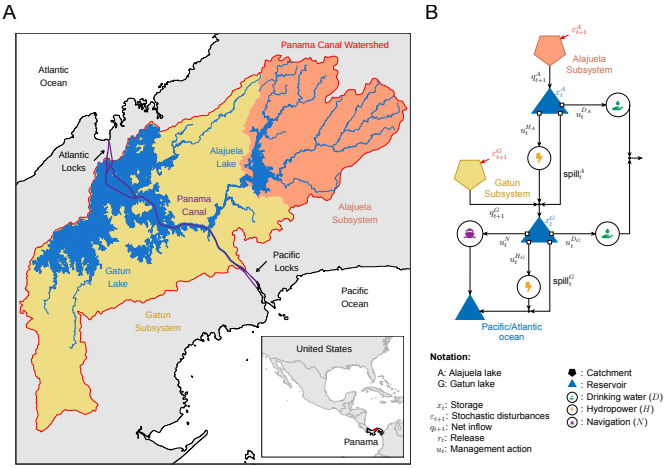
Which economies use the Panama Canal?

Routes	PCU/MS 2023	PCU/MS 2024	% Δ PCU/MS
East Coast U.S. - Asia	246,768,488	204,056,339	-17.31%
East Coast U.S. - W.C. South America	48,063,058	36,621,051	-23.81%
South America Intercoastal	26,037,602	30,509,715	17.18%
Europe - West Coast South America	25,799,446	20,293,355	-21.34%
East Coast U.S. - W.C. Central America	19,685,783	19,042,652	-3.27%
Europe - West Coast U.S.	15,457,079	14,181,845	-8.25%
U.S. Intercoastal including Alaska and Hawaii	11,884,991	13,580,741	14.27%
Central America Intercoastal	8,797,454	9,432,120	7.21%
E.C. Central America - W.C. South America	9,509,440	9,255,494	-2.67%
E.C. South America - Asia	16,336,445	7,944,913	-51.37%
E.C. South America - W.C. Central America	7,632,903	6,776,150	-11.22%
E.C. South America - West Coast U.S.	6,229,097	5,422,850	-12.94%
Asia - E.C. Central America	7,730,648	5,046,868	-34.72%
East Coast U.S. - Oceania	5,942,570	4,639,835	-21.92%
West Indies - Asia	5,164,159	3,979,433	-22.94%
W.C. Central America - Europe	3,016,240	2,960,520	-1.85%
Europe - Oceania	2,564,343	1,359,786	-46.97%
Asia - Europe	2,015,420	1,236,419	-38.65%
E.C. Central America - West Coast US	2,201,127	1,210,800	-44.99%
All Other Routes	40,300,417	25,542,186	-36.62%
Total	**511,136,710**	**423,093,072**	

Source: Panama Canal, Transit statistics. Panama Canal Universal Measurement System (PC/UMS)

back

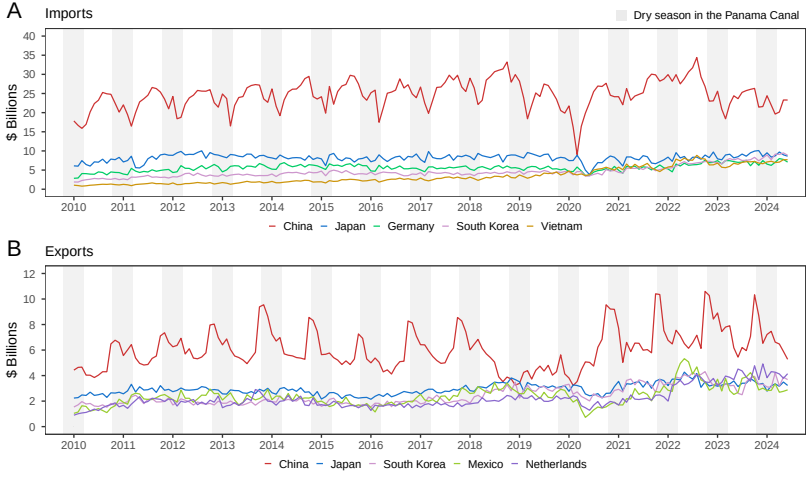
Schematic of the Panama Canal system



Source: [Prieto et al., 2026]

back

US imports and exports



back

AIS Traffic Calibration: Robustness

	(1) Baseline	(2) + PC controls	(3) + MR controls	(4) Preferred
Days below 82 ft × Panama	−0.0032**	−0.0036***	−0.0146	−0.0109**
	(0.0015)	(0.0010)	(0.0097)	(0.0050)
Days above 86 ft × Panama	0.0028**	0.0021**	−0.0007	0.0081
	(0.0014)	(0.0009)	(0.0048)	(0.0050)
OD × gate FE	Yes	Yes	Yes	Yes
Time FE	Yes	Yes	–	–
Origin × time FE	–	–	Yes	Yes
Destination × time FE	–	–	Yes	Yes
Panama-specific year controls	–	Yes	–	Yes
Panama-specific month controls	–	Yes	–	Yes
Observations	2,941,286	2,941,286	2,941,286	2,941,286

Notes: PPML estimates on a common estimation sample. Driscoll–Kraay SEs (L=6). Column (4) is the preferred specification used to calibrate the Panama transport-cost shock. $^{*}p < 0.10$, $^{**}p < 0.05$, $^{***}p < 0.01$.

back

Hat Algebra: Solving the Counterfactual

- **Counterfactual cost shock:** $\hat{t}_{ll'} = \exp(\delta_R \Delta\omega\, \kappa^{PC}_{ll'})$
- **Fixed-point system** (solve for $\hat{p}_l$, $\hat{\pi}_l$):

$$\hat{p}_l = \sum_{l' \in \mathcal{V}} s_{l'l}\, \hat{t}_{l'l}^{-\theta}\, \hat{p}_{l'} + b_l^{\tilde{P}}(\hat{\boldsymbol{\pi}}) \qquad \hat{\pi}_l = \sum_{l' \in \mathcal{V}} s_{ll'}\, \hat{t}_{ll'}^{-\theta}\, \hat{\pi}_{l'} + b_l^{\tilde{\Pi}}(\hat{\mathbf{p}}, \hat{\boldsymbol{\pi}})$$

where $\hat{p}_l$ and $\hat{\pi}_l$ are the consumer-side and producer-side network potentials; $s_{ll'}$ is the baseline traffic shares; $b_l^{\tilde{P}}$, $b_l^{\tilde{\Pi}}$ capture local expenditure and income contributions; $b_l = 0$ for transit nodes $l \in \mathcal{V}_M$.

- **Recover counterfactual objects:**

Welfare

$$\hat{W}_i = \hat{\Pi}_i^{-\theta/(\theta+1)} / \hat{P}_i$$

Traffic

$$\hat{\Xi}_{ll'} = \hat{t}_{ll'}^{-\theta} \hat{P}_l^{-\theta} \hat{\Pi}_{l'}^{-\theta}$$

Trade flows

$$X'_{ij} = Y_i \left[\mathbf{D}^{X'} - \hat{\boldsymbol{\Xi}} \right]^{-1}_{ij} E_j$$

back

Low-Water Effects: Rainfall Instruments

	Transits (ships/mth)	Volume (tons/mth)	Toll revenue (USD/mth)	Rev/Transit (USD/ship)	Slots available (slots/mth)
Days below 82 ft	−0.0040**	−0.0091***	−0.0042**	−0.0002	−0.0073**
	(0.0022)	(0.0030)	(0.0019)	(0.0013)	(0.0020)
Below 82 ft (% change)					
+10 days	-3.91	-8.67	-4.08	-0.19	-6.99
+30 days	-11.28	-23.82	-11.76	-0.57	-19.55
AR p-value	0.0176	0.0037	0.0405	0.9288	0.0111
HAC KP F	6.44	6.44	6.44	6.44	6.44
Observations	256	256	256	256	256

Notes: All dependent variables are in logs. Reference regime: lake levels at or above 82 ft; the separate high-water effect is fixed at zero. Instruments are accumulated rainfall deficits over preceding months 1–6 and 7–12. All models include month and year fixed effects. Parentheses report conventional Newey–West HAC standard errors ($L = 4$); brackets report 95% weak-IV-robust Anderson–Rubin confidence sets. Stars use HAC Anderson–Rubin tests under the maintained instrument restrictions: $^{*}p < 0.10$, $^{**}p < 0.05$, $^{***}p < 0.01$. Percentage effects are $100[\exp(d\hat{\beta}) - 1]$.

back

Low-Water Effects: Inflow Instruments

	Transits (ships/mth)	Volume (tons/mth)	Toll revenue (USD/mth)	Rev/Transit (USD/ship)	Slots available (slots/mth)
Days below 82 ft	−0.0057*	−0.0112**	−0.0055***	0.0003	−0.0082**
	(0.0026)	(0.0039)	(0.0025)	(0.0017)	(0.0023)
Below 82 ft (% change)					
+10 days	-5.57	-10.58	-5.30	0.27	-7.90
+30 days	-15.79	-28.49	-15.08	0.81	-21.88
AR p-value	0.0547	0.0122	0.0005	0.2307	0.0154
HAC KP F	5.24	5.24	5.24	5.24	5.24
Observations	256	256	256	256	256

Notes: Dependent variables are in logs. Reference regime: lake levels at or above 82 ft; the separate high-water effect is fixed at zero. Instruments: accumulated Gatún inflow volumes over preceding months 1–6 and 7–12. Month and year fixed effects included. Parentheses report conventional Newey–West HAC standard errors ($L = 4$); brackets report 95% weak-IV-robust Anderson–Rubin confidence sets. Stars use HAC Anderson–Rubin tests under the maintained instrument restrictions: $^{*}p < 0.10$, $^{**}p < 0.05$, $^{***}p < 0.01$. Percentage effects are $100[\exp(d\hat{\beta}) - 1]$.

back

References I


Allen, T. and Arkolakis, C. (2022).
The welfare effects of transportation infrastructure improvements.
The Review of Economic Studies, 89(6):2911–2957.


Bekkers, E., Francois, J. F., and Rojas-Romagosa, H. (2018).
Melting ice caps and the economic impact of opening the northern sea route.
The Economic Journal, 128(610):1095–1127.


BTS, B. (2024).
U.S. Trade and the Impact of Low Water Levels in Gatun Lake and the Panama Canal.
Technical report, U.S. Department of Transportation.


Cruz, J. L. and Rossi-Hansberg, E. (2024).
The economic geography of global warming.
Review of Economic Studies, 91(2):899–939.


Dell, M., Jones, B. F., and Olken, B. A. (2012).
Temperature shocks and economic growth: Evidence from the last half century.
American Economic Journal: Macroeconomics, 4(3):66–95.

References II



Dunbar, G., Steingress, W., and Tomlin, B. (2023).
Climate variability and international trade.
Technical report, Bank of Canada Staff Working Paper.



Feng, A., Li, H., and Wang, Y. (2025).
We are all in the same boat: Cross-border spillovers of climate shocks through international trade and supply chains.
The Economic Journal, 135(669):1433–1466.



Gouel, C. and Laborde, D. (2021).
The crucial role of domestic and international market-mediated adaptation to climate change.
Journal of Environmental Economics and Management, 106:102408.



Hanson, S. E. and Nicholls, R. J. (2020).
Demand for ports to 2050: Climate policy, growing trade and the impacts of sea-level rise.
Earth's Future, 8(8):e2020EF001543.



Heiland, I., Moxnes, A., Ulltveit-Moe, K. H., and Zi, Y. (2025).
Trade from space: Shipping networks and the global implications of local shocks.
Review of Economics and Statistics, pages 1–45.

References III

Känzig, D. R. and Raghavan, R. (2025).
The macroeconomic effects of supply chain shocks: Evidence from global shipping disruptions.
Unpublished manuscript.

Muñoz, S. E., Lawrence, L., and Wang, S. (2025).
Drying of the Panama Canal in a warming climate.
Geophysical Research Letters, 52(18):e2025GL117038.

Nath, I. (2025).
Climate change, the food problem, and the challenge of adaptation through sectoral reallocation.
Journal of Political Economy, 133(6):1705–1756.

PCA, P. (2026).
Maritime services: Advisory to shipping.

Prieto, J., Galelli, S., and Ortiz-Bobea, A. (2026).
Recovering revealed preferences of centralized decision-makers: Evidence from water allocation in the panama canal.
SSRN Working Paper.

Rudik, I., Lyn, G., Tan, W., and Ortiz-Bobea, A. (2022).
The economic effects of climate change in dynamic spatial equilibrium.

References IV



Shen, G., Yan, X., Zhou, L., and Wang, Z. (2020).
Visualizing the USA's maritime freight flows using DM, LP, and AON in GIS.
ISPRS International Journal of Geo-Information, 9(5):286.



UNCTAD (2024).
Review of Maritime Transport 2024.
United Nations, 2024 edition.